

Cite this: *Chem. Sci.*, 2019, 10, 8668

All publication charges for this article have been paid for by the Royal Society of Chemistry

# Canonical DNA minor groove insertion of bisbenzamidine–Ru(II) complexes with chiral selectivity†

Mateo I. Sánchez,<sup>a</sup> Gustavo Rama,<sup>b</sup> Renata Calo-Lapido,<sup>a</sup> Kübra Ucar,<sup>c</sup> Per Lincoln,<sup>c</sup> Miguel Vázquez López,<sup>b</sup> Manuel Melle-Franco,<sup>d</sup> José L. Mascareñas<sup>b\*</sup> and M. Eugenio Vázquez<sup>b\*</sup>

We report the first Ru(II) coordination compounds that interact with DNA through a canonical minor groove insertion mode and with selectivity for A/T rich sites. This was made possible by integrating a bis-benzamidine minor groove DNA-binding agent with a ruthenium(II) complex. Importantly, one of the enantiomers ( $\Delta$ -[Ru(bpy)<sub>2</sub>b4bpy]<sup>2+</sup>,  $\Delta$ -4Ru) shows a considerably higher DNA affinity than the parent organic ligand and the other enantiomer, particularly for the AATT sequence, while the other enantiomer preferentially targets long AAATTT sites with overall lower affinity. Finally, we demonstrate that the photophysical properties of these new binders can be exploited for DNA cleavage using visible light.

Received 20th June 2019

Accepted 30th July 2019

DOI: 10.1039/c9sc03053k

rsc.li/chemical-science

## Introduction

Over the past few decades there has been great interest in the development of transition metal complexes that target DNA as antitumor agents.<sup>1</sup> In this context, intercalative ruthenium(II) complexes are particularly attractive due to their good kinetic stability, as well as their rich redox and photochemistry.<sup>2</sup> These complexes typically contain two bipyridine ligands, and one large heteroaromatic unit that penetrates into DNA through the major groove and stacks between consecutive base pairs.<sup>3</sup> Unfortunately, just like polycyclic organic intercalators,<sup>4</sup> these complexes display poor sequence selectivity with preference for G/C-rich sequences. In contrast, organic minor groove DNA-binding agents typically show good discrimination between binding sites.<sup>5</sup> Although minor groove contacts have been proposed for a number of coordination compounds,<sup>6</sup> to our knowledge, a canonical minor groove binding complex that inserts one of its ligands into the DNA minor groove has not yet been demonstrated.<sup>7</sup>

We reasoned that in the same way polyaromatic ligands, such as dpqn, dppz or dpq, define the intercalative binding mode of traditional DNA-binding metal complexes,<sup>8</sup> engineering an organic minor groove binder as a metal ligand could yield complexes capable of inserting into the minor groove of DNA, and thus display new DNA binding properties not observed with traditional metallointercalators.<sup>9,10</sup> More specifically, we considered the use of aza-bisbenzamidines as model minor groove binders, owing to their synthetic accessibility and their well-established fluorogenic properties.<sup>11</sup> This type of compound tends to insert into the minor groove of A/T rich sequences with dissociation constants in the low  $\mu$ M range.<sup>12</sup> Herein we describe the synthesis of several ruthenium(II) complexes incorporating bis-(methylamino-benzamidine)-2,2'-bipyridine ligands, and demonstrate that they bind to A/T-rich DNA sequences by insertion of such a benzamidine ligand into the minor groove. Importantly, we also found that the DNA binding profile of these complexes is heavily dependent on their chirality, which not only affects their overall binding affinity, but also determines their preferred binding sequence.

## Results and discussion

### Synthesis and characterization of the bisbenzamidine complexes

The aza-bisbenzamidine ligands and their corresponding complexes were synthesized as shown in Scheme 1.<sup>11</sup> Thus, reductive amination of 2,2'-bipyridine-4,4'-dicarbaldehyde (**1a**, Scheme 1), with commercially available 4-aminobenzene carboximidamide dihydrochloride, afforded the desired bis-benzamidine-bipyridine ligand **b4bpy** in good yield.<sup>22</sup> The reaction of this ligand with each of the enantiopure Hua and

<sup>a</sup>Centro Singular de Investigación en Química Biolóxica e Materiais Moleculares (CiQUS), Departamento de Química Orgánica, Universidade de Santiago de Compostela, 15782 Santiago de Compostela, Spain. E-mail: eugenio.vazquez@usc.es

<sup>b</sup>Centro Singular de Investigación en Química Biolóxica e Materiais Moleculares (CiQUS), Departamento de Química Inorgánica, Universidade de Santiago de Compostela, 15782 Santiago de Compostela, Spain

<sup>c</sup>Department of Chemistry and Chemical Engineering, Chalmers University of Technology, SE 412 96 Gothenburg, Sweden

<sup>d</sup>Ciceco - Aveiro Institute of Materials, University of Aveiro Campus Universitario de Santiago, Aveiro, 3810-193, Portugal

† Electronic supplementary information (ESI) available. See DOI: 10.1039/c9sc03053k



von Zelewsky's reagents,  $\Lambda$ - and  $\Delta$ -*cis*-[Ru(bpy)<sub>2</sub>(py)<sub>2</sub>]<sup>2+</sup>,<sup>13</sup> afforded the enantiomeric complexes  **$\Lambda$ -4Ru** ( $\Lambda$ -[Ru(bpy)<sub>2</sub>**b4bpy**]<sup>2+</sup>) and  **$\Delta$ -4Ru** ( $\Delta$ -[Ru(bpy)<sub>2</sub>**b4bpy**]<sup>2+</sup>), respectively. The same sequence of transformations starting with 2,2'-bipyridine-5,5'-dicarbaldehyde (**1b**, Scheme 1) leads to the regioisomeric complexes  **$\Lambda$ -5Ru** ( $\Lambda$ -[Ru(bpy)<sub>2</sub>**b5bpy**]<sup>2+</sup>) and  **$\Delta$ -5Ru** ( $\Delta$ -[Ru(bpy)<sub>2</sub>**b5bpy**]<sup>2+</sup>), also in good yields (Scheme 1).

The CD spectra of both  $\Lambda$ -complexes ( **$\Lambda$ -4Ru** and  **$\Lambda$ -5Ru**) are dominated by a large LC transition band with a positive Cotton effect at 285–310 nm and a broad and less intense metal-to-ligand charge transfer (MLCT) band centered at *ca.* 460 nm, also displaying positive Cotton effects. These features are consistent with the  $\Lambda$ -configuration around the metal center in octahedral coordination compounds.<sup>14</sup> Likewise, their enantiomeric complexes ( **$\Delta$ -4Ru** and  **$\Delta$ -5Ru**) display mirror image CD spectra with negative Cotton effects (see the ESI†).

### DNA binding of the bisbenzamidine–Ru(II) complexes

Having the two pairs of enantiomeric complexes at hand, we studied their DNA binding properties by taking advantage of the intrinsic fluorogenic properties of the ruthenium(II) polypyridyl complexes.<sup>15</sup> Thus, successive aliquots of a 250  $\mu$ M solution of a short double stranded hairpin oligonucleotide containing an extended six-base-pair A/T-rich binding site (**A3T3**) were added to a 0.5  $\mu$ M solution of  **$\Lambda$ -4Ru** in Tris–HCl buffer and the luminescence emission spectra upon irradiation at the benzamidine excitation wavelength (329 nm) were recorded after each addition. This resulted in a series of spectra displaying a progressive increase in the emission intensity of the  **$\Lambda$ -4Ru** <sup>3</sup>MLCT band at 605 nm, which could be fitted to a one to one binding model including contribution from non-specific binding, with a dissociation constant of  $K_D \approx 0.62 \mu$ M

(Fig. 1a and Table 1, see the ESI† for details about curve fitting analysis).<sup>16</sup> Titrations with other DNA oligonucleotides exhibiting five (**A2T3**) and four (**A2T2**) consecutive A/T base pairs resulted in progressively weaker binding. Not surprisingly,  **$\Lambda$ -4Ru** displayed considerably lower affinity for a G/C-rich oligo (**G2C3**). Similar experiments were carried out with the enantiomeric complex  **$\Delta$ -4Ru**, the isomeric  **$\Lambda$ -5Ru** and  **$\Delta$ -5Ru** complexes, and the parent bis-benzamidine ligands (**b4bpy** and **b5bpy**,  $\lambda_{exc} = 329$  nm;  $\lambda_{em} = 389$  nm). The resulting apparent dissociation constants are summarized in Table 1 and graphically compared in Fig. 1b.

The ligand **b5bpy** and its derivatives  **$\Lambda$ -5Ru** and  **$\Delta$ -5Ru** display lower affinity than its **b4bpy** counterparts. The reduced binding of **b5bpy** probably arises from its linear structure, which cannot simultaneously optimize the interactions of the two amidinium groups with the bottom of the DNA minor groove.<sup>12,17,18</sup> Moreover,

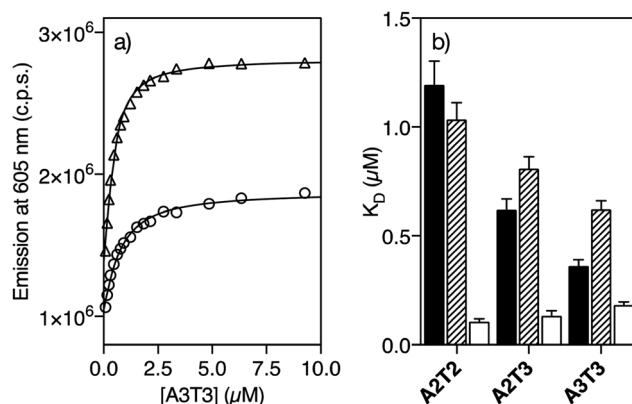
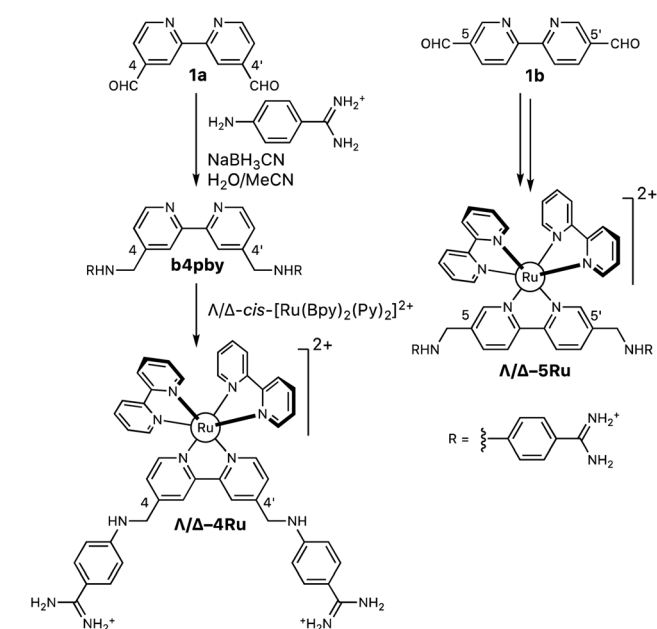


Fig. 1 (a) Representative titration profiles of 0.5  $\mu$ M solutions of  **$\Lambda$ -4Ru** (○) and  **$\Delta$ -4Ru** (Δ) complexes with increasing concentration of the oligo **A3T3**. (b) Dissociation constants of **b4bpy** (black),  **$\Lambda$ -4Ru** (striped), and  **$\Delta$ -4Ru** (white) with a set of A/T-rich oligonucleotides. Hairpin sequences (binding sites in *italics*): **A3T3**: 5'-GGC *AAATTT* CAG T<sub>5</sub> CTG *AAATTT* GCC-3'; **A2T3**: 5'-GGCG *AATTT* CGC T<sub>5</sub> GCG *AAATT* CGCC-3'; **A2T2**: 5'-GGCG *AATT* CAGC T<sub>5</sub> GCTG *AATT* CGCC-3'/A/T-rich binding sites, and the central hairpin loop (T<sub>5</sub>) is shown in *italics*. All titrations were performed in 20 mM Tris–HCl buffer with 100 mM NaCl, pH 7.5, at 298 K.

Table 1 Binding constants for the bipyridine-benzamidine ligands and their ruthenium(II) coordination complexes<sup>a</sup>

	A2T2	A2T3	A3T3	G2C3
<b>b4bpy</b>	1.19 (0.11)	0.62 (0.05)	0.36 (0.03)	n.b.
<b>b5bpy</b>	2.58 (0.58)	1.29 (0.15)	0.84 (0.07)	n.b.
<b><math>\Delta</math>-4Ru</b>	<b>0.11 (0.01)</b>	0.13 (0.02)	0.18 (0.01)	1.69 (0.09)
<b><math>\Lambda</math>-4Ru</b>	<b>1.04 (0.08)</b>	0.81 (0.06)	0.62 (0.04)	2.64 (0.28)
<b><math>\Delta</math>-5Ru</b>	4.24 (0.49)	3.64 (0.26)	3.08 (0.16)	4.90 (0.05)
<b><math>\Lambda</math>-5Ru</b>	4.04 (0.76)	3.81 (0.76)	3.24 (0.28)	3.63 (0.39)

<sup>a</sup>  $K_D$  ( $\mu$ M) was measured in 20 mM Tris–HCl buffer with 100 mM NaCl, pH 7.5, at 298 K and calculated from three independent titrations. The estimated  $K_D$  error is shown in brackets. n.b. indicates that no binding was observed under the experimental conditions used in the titrations. Hairpin oligonucleotide sequence of **G2C3**: 5'-GGCA *GGCC* CAGC T<sub>5</sub> GCTG *GGCC* TGCC-3'.



Scheme 1 Synthesis of the set of  $\Lambda$ - and  $\Delta$ -bisbipyridyl ruthenium(II) complexes containing the ligands **b4bpy** and **b5bpy**.

$\Delta$ -5Ru and  $\Delta$ -5Ru showed weaker DNA binding than **b5bpy**, regardless of the chirality of the metal center. On the other hand, the ligand **b4bpy** and  $\Delta$ -4Ru display comparable binding affinities and a clear preference for those DNAs featuring longer A/T sites, so titrations with oligos exhibiting six (**A3T3**), five (**A2T3**), and four (**A2T2**) consecutive A/T base pairs resulted in progressively weaker dissociation constants (Table 1 and Fig. 1b). Remarkably,  $\Delta$ -4Ru displays much higher affinity for all the above A/T-rich DNAs than **b4bpy** or  $\Delta$ -4Ru, particularly for **A2T2** ( $K_D = 0.11 \mu\text{M}$ , Table 1). Indeed, its interaction with the **A2T2** oligo is over 10 times stronger than that of its enantiomer  $\Delta$ -4Ru, or that of the parent organic ligand **b4bpy**. Hence, proper ligand engineering allowed transforming a weak and nonspecific DNA binder, such as  $[\text{Ru}(\text{bpy})_3]^{2+}$  into complexes capable of inserting into the minor groove of specific DNA sequences with high affinity. Curiously, in the case of the isomer **b5bpy**, the metal coordination has a negative effect on the affinity (e.g.,  $\Delta/\Delta$ -5Ru vs. **b5bpy**).

### DNA binding occurs through insertion into the DNA minor groove

In order to confirm that the interaction of  $\Delta$ -4Ru with the target DNA occurs by insertion into the minor groove, we measured the circular dichroism spectra of the oligonucleotide **A3T3** in the presence of increasing concentrations of the ligand **b4bpy**,  $\Delta$ -4Ru, and  $\Delta$ -4Ru. Incubation with **b4bpy** resulted in the appearance of a positive induced CD band at ca. 345 nm, consistent with its insertion into the DNA minor groove (Fig. 2a).<sup>20,21</sup> Importantly, mixing the DNA with either  $\Delta$ -4Ru or  $\Delta$ -4Ru produced a similar induced CD band, although with reduced intensity compared to that of the free ligand **b4bpy**, perhaps due to the conformational restrictions imposed by coordination to the metal ion (Fig. 2b). The observation of this induced CD band, which arises from a chiral twisting of the bis-benzamidine ligand, supports the formation of DNA complexes of similar nature to those formed with **b4bpy**.<sup>22</sup>

Fluorescence competition assays show that  $\Delta$ -4Ru displaces DAPI (4,6-diamidino-2-phenylindole) and Hoechst 33258, typical A/T-rich minor groove binders, very efficiently,<sup>23</sup> thus reinforcing the hypothesis that these complexes insert into the DNA minor groove (Fig. 2c and S10 in the ESI†).<sup>24</sup> Linear Dichroism (LD) experiments, which provide information about the orientation of the bound complexes with respect to the DNA,<sup>25</sup> were also consistent with minor groove insertion. Thus, the LD spectra of a reference intercalative complex  $\Delta$ -[Ru(bpy)<sub>2</sub>phen]<sup>2+</sup> show a strong positive LD signal in the B(E)-polarized MLCT band at 440 nm, arising from the placement of the phen ligand almost coplanar to the DNA base pairs and the complex two-fold symmetry axis slightly rotated clockwise (by about 10°) from the ideal intercalation geometry. This arrangement results in a decreased LD at 440 nm for its enantiomer  $\Delta$ -[Ru(bpy)<sub>2</sub>phen]<sup>2+</sup> (Fig. 2d).<sup>26,29</sup> By substituting the intercalative phen ligand with the minor groove binder **b4bpy**, the  $\Delta$ -4Ru enantiomer now shows a more negative LD band compared to  $\Delta$ -4Ru, which is unprecedented among mononuclear ruthenium polypyridyl complexes. This inversion in the relative intensities is consistent with the alignment of the

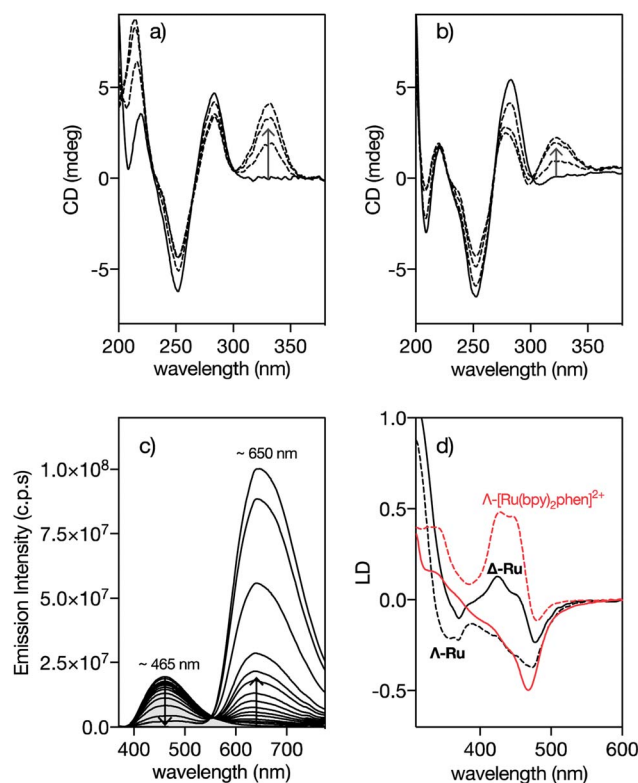


Fig. 2 Circular Dichroism spectra of 5  $\mu\text{M}$  solutions of the **A3T3** oligo in 20 mM Tris-HCl buffer with 100 mM NaCl, pH 7.5 (solid lines) in the presence of 1, 3 and 5 eq. of (a) **4bpy** and (b)  $\Delta$ -4Ru showing the induced CD band at ca. 330 nm corresponding to the benzamidine chromophore. **A3T3**: 5'-GGC AAATTT CAG T<sub>5</sub> CTG AAATTT GCC-3'; A/T-rich binding sites and the central hairpin loop (T<sub>5</sub>) are shown in italics. The CD spectra obtained upon incubation of the  $\Delta$ -4Ru isomer with the **A3T3** DNA are qualitatively the same as those for the enantiomeric  $\Delta$ -4Ru; (c) DAPI displacement assay showing a series of emission spectra of a mixture of 0.25  $\mu\text{M}$  DAPI and 0.5  $\mu\text{M}$  **A2T2** in the presence of increasing concentration of  $\Delta$ -4Ru; (d) Linear dichroism (LD) spectra of flow-oriented calf thymus DNA with the two enantiomers of **4Ru** (black lines, P/Ru = 20) and [Ru(bpy)<sub>2</sub>phen]<sup>2+</sup> (red lines, P/Ru = 30) in 10 mM NaCl.<sup>29</sup>  $\Delta$ -enantiomers as dashed lines and  $\Delta$ -enantiomers as solid lines in both cases. Spectra are normalized to A = 1 for the long wavelength absorption maximum of the free complex. The LD spectra are further normalized to perfect orientation ( $S = 1$ ) by setting the LD<sup>r</sup> value at the DNA band at 260 nm to  $-1.5$ .<sup>29</sup>

substituted **4bpy** ligand in the direction of the DNA minor groove, and a counter-clockwise rotation of the complex from the ideal intercalation geometry by about 45°, moving the B(E) transition away from the helix axis and consequently giving rise to a decreased, or even negative, LD at 440 nm.

### Computational modeling of the interaction

To gain some structural insight into the interaction of our molecules with the DNA, we performed modelling studies using previously tested docking procedures<sup>27</sup> and taking as reference the high-resolution crystal structure of the Dickerson-Drew dodecamer, which features a short A/T-rich binding site in the middle of its sequence (5'-CGCGAATTCGCG-3', **xA2T2**).<sup>28</sup> The lowest energy docking poses of the complexes  $\Delta$ -Ru and  $\Delta$ -4Ru





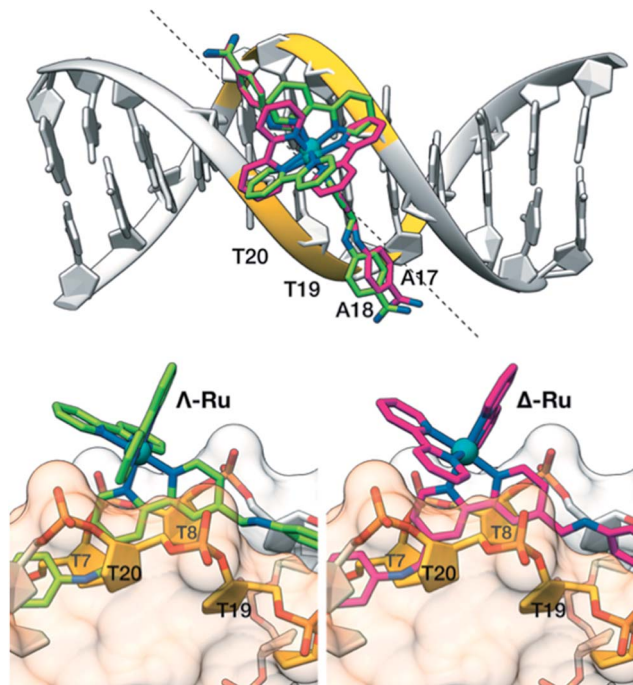


Fig. 3 Docking structures of  $\Delta$ -Ru (green) and  $\Delta$ -4Ru (magenta). Top view: alignment of the b4bpy ligands with the minor groove in the Dickerson–Drew dodecamer (xA2T2). The dashed line forms a 45° angle with the DNA axis and matches the approximate orientation of the b4bpy ligand in the complexes. Bottom left: side view of  $\Delta$ -Ru showing the bipyridine ligand between the phosphate groups flanking T20 (front, light orange surface) and T8 (back, light grey surface). Bottom right: the same view of  $\Delta$ -Ru.<sup>33</sup>

on this DNA present the bisbenzamidinium ligand inserted into the minor groove in the A/T-rich region of the oligonucleotide.

More importantly, the bulkier bipyridine ligands match the indentations between the T7–T8/T19–T20 phosphate groups in the DNA backbone (Fig. 3), allowing the benzamidinium ligand to reach the bottom of the DNA minor groove. Docking studies with a different model DNA based on fiber diffraction data (fA2T2)<sup>30</sup> resulted in most populated poses qualitatively similar to those observed with xA2T2. Importantly, the binding energies resulting from the docking experiments are highly dependent on the DNA model used in the calculations. Thus, the intermolecular binding energies obtained with the DNA fA2T2 were  $-16.5$  and  $-15.6$  kcal mol<sup>-1</sup> for  $\Delta$ -4Ru and  $\Delta$ -Ru respectively, in line with the observed experimental difference in the binding affinity. However, the interaction energy with xA2T2 turned out to be about  $-20$  kcal mol<sup>-1</sup> for both isomers. Summing up, these docking studies support the minor groove binding mode for both  $\Delta$ -4Ru and  $\Delta$ -Ru and also suggest that the strength and sequence selectivity are highly dependent on the microstructure of the DNA substrates, as previously reported for related minor groove binders.<sup>31</sup> The shape complementarity with the DNA minor groove plays a key role in the strength of the binding, as well as in the sequence discrimination between both enantiomeric forms, which ultimately appears to be related to the way in which the accessory bipyridine ligands match the DNA backbone.<sup>32</sup> Taken

together, these experimental and computational data demonstrate that through proper ligand engineering it is possible to obtain metal complexes that selectively recognize DNA through a canonical minor groove insertion mechanism.

### Study of the bisbenzamidinium-Ir(III) analogs $\Delta$ -4Ir and $\Lambda$ -4Ir

We also studied the DNA binding of the 2-phenylpyridine cyclometalated iridium(III) complexes containing the minor groove binding ligand b4bpy. These monocationic complexes have roughly the same geometry as dicationic ruthenium(II) complexes, but lower charge (+1). Thus we synthesized the complexes  $\Delta$ - and  $\Lambda$ -[Ir(ppy)<sub>2</sub>b4bpy]<sup>+</sup> ( $\Delta$ -4Ir and  $\Lambda$ -4Ir respectively; ppy = 2-phenylpyridine), by reaction of b4bpy with a dimeric bis(2-phenylpyridinato) iridium chloride precursor [(ppy)<sub>2</sub>Ir( $\mu$ -Cl)]<sub>2</sub>, followed by HPLC resolution of the resulting enantiomeric mixture (see the ESI†).<sup>34</sup>

The interaction of these complexes with DNA was studied by steady-state luminescence titrations monitoring the emission from the complexes at 575 nm upon irradiation of the benzamidinium fluorophore at 329 nm (ESI†). As shown in Table 2, both  $\Delta$ -4Ir and  $\Lambda$ -4Ir display similar trends to  $\Delta$ -4Ru and  $\Lambda$ -4Ru, although with slightly reduced affinities, which might be likely related to the lower charge of these complexes. Thus, for example,  $\Delta$ -4Ir also displays higher affinity for A2T2 than  $\Lambda$ -4Ir. Interestingly, the two iridium isomers show different sequence selectivity, so while the affinity of  $\Delta$ -4Ir for DNA is higher for shorter A/T-tracts,  $\Lambda$ -4Ir shows a marked preference for longer

Table 2 Binding constants for the bipyridine-benzamidinium iridium(III) complexes<sup>a</sup>

	A2T2	A2T3	A3T3	G2C3
b4bpy	1.19 (0.11)	0.62 (0.05)	0.36 (0.03)	n.b.
$\Delta$ -4Ir	0.27 (0.09)	0.49 (0.03)	1.01 (0.12)	1.44 (0.09)
$\Lambda$ -4Ir	1.15 (0.13)	0.62 (0.04)	0.47 (0.03)	0.70 (0.05)

<sup>a</sup>  $K_D$  ( $\mu$ M) was measured in 20 mM Tris–HCl buffer with 100 mM NaCl, pH 7.5, at 298 K and calculated from three independent titrations. The estimated  $K_D$  error is shown in brackets. n.b. if no significant binding is observed.

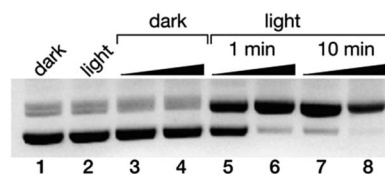


Fig. 4 Ethidium bromide-stained agarose gels (0.7%) of the photocleavage of 25 ng  $\mu$ L<sup>-1</sup> pCDNA3.1(+) in 20 mM Tris–HCl buffer with 100 mM NaCl, pH 7.5, with  $\Delta$ -4Ru. All lanes contain the plasmid pCDNA3.1(+); lane 1: plasmid in the absence of  $\Delta$ -4Ru in the dark; lane 2, the same plasmid after 10 min of irradiation in the absence of the  $\Delta$ -4Ru complex; lanes 3 and 4: 20 and 100  $\mu$ M  $\Delta$ -4Ru in the dark; lanes 5 and 6: 20 and 100  $\mu$ M  $\Delta$ -4Ru irradiated for 1 min; lanes 7 and 8: 20 and 100  $\mu$ M  $\Delta$ -4Ru irradiated for 10 min. Irradiation was performed with a Thorlabs M455L3 Royal Blue (455 nm) Mounted High-Power LED, 1000 mA, using a custom made setup (see the ESI†).



A/T-rich sites. Curiously, the affinity for G/C-rich oligos is higher than for the ruthenium analogs.

### Photo-endonuclease activity of $\Delta$ -4Ru

Finally, we studied the potential application of these newly developed DNA minor groove binders as photo-endonucleases. It is known that irradiation of trisbipyridyl Ru(II) complexes gives rise to a <sup>3</sup>MLCT (metal-to-ligand charge transfer) excited state that can act as a photosensitizer to generate singlet oxygen (<sup>1</sup>O<sub>2</sub>),<sup>35</sup> which ultimately leads to DNA strand breaks.<sup>36</sup> Thus, a 50 ng  $\mu$ L<sup>-1</sup> solution of the pCDNA3.1(+) plasmid was incubated with increasing concentration of the complex  $\Delta$ -4Ru (20 and 100  $\mu$ M) and irradiated with a 455 nm LED source for either 5 or 10 min, and the resulting mixtures were analyzed by agarose electrophoresis. As expected, in the absence of light,  $\Delta$ -4Ru was inert, and no new bands indicating the degradation of the pCDNA3.1(+) plasmid were observed. However, the irradiated solutions displayed new bands in the agarose gel consistent with the illumination time and a concentration-dependent scission of the plasmid (Fig. 4). It is important to note that the parent ruthenium complex [Ru(bpy)<sub>3</sub>]<sup>2+</sup> does not induce the light-promoted DNA cleavage, as it is not capable of interacting with DNA.

## Conclusions

In summary, ruthenium(II) coordination complexes containing a designed bis-benzamidine ligand selectively bind to A/T-rich sequences in DNA by means of a classic minor groove insertion mechanism. To our knowledge, this type of interaction has not been demonstrated for metal-based DNA-binding agents. Importantly, the two enantiomers display markedly different DNA binding properties, so  $\Delta$ -4Ru binds more strongly than  $\Lambda$ -4Ru to all the studied DNA sites and preferentially to those with a short A/T site (AATT) with ~10-fold higher affinity than  $\Lambda$ -4Ru. In contrast the  $\Lambda$ -4Ru isomer preferentially binds to DNA with longer A/T sites (A3T3) and shows only residual binding affinity for the shorter DNA A2T2 preferred by its enantiomer. Finally,  $\Delta$ -4Ru exhibited efficient nuclease activity upon irradiation, which might find applications in photodynamic therapy.

## Conflicts of interest

There are no conflicts to declare.

## Acknowledgements

Financial support from the Spanish grants CTQ2015-70698-R, SAF2016-76689-R and Orfeo-cinca network CTQ2016-81797-REDC; the Ministerio de Ciencia, Innovación y Universidades of Spain, RTI2018-099877-B-I00; the Xunta de Galicia (2015-CP082, ED431C 2017/19, Centro singular de investigación de Galicia accreditation 2016–2019, ED431G/09), the European Union (European Regional Development Fund – ERDF), and the European Research Council (Advanced Grant No. 340055) are gratefully acknowledged. We also acknowledge the support from the Portuguese Foundation for Science and Technology, FCT, (IF/

00894/2015) and CICECO – Aveiro Institute of Materials, FCT Ref. UID/CTM/50011/2019, financed by national funds through the FCT/MCTES. M. E. V. also acknowledges the support of the Fundación Asociación Española Contra el Cáncer (AECC) (IDE-AS197VAZQ grant). We also thank A. Arda and J. Jiménez-Barbero (CIC bioGUNE) for carrying out the preliminary spectroscopic characterization.

## References

- (a) K. L. Haas and K. J. Franz, *Chem. Rev.*, 2009, **109**, 4921–4960; (b) P. C. A. Bruijninx and P. J. Sadler, *Curr. Opin. Chem. Biol.*, 2008, **12**, 197–206; (c) M. A. Jakupc, M. Galanski, V. B. Arion, C. G. Hartinger and B. K. Keppler, *Dalton Trans.*, 2008, 183–194; (d) J. K. Barton, *Science*, 1986, **233**, 727–734.
- (a) B. M. Zeglis, V. C. Pierre and J. K. Barton, *Chem. Commun.*, 2007, 4565–4579; (b) M. R. Gill, J. Garcia-Lara, S. J. Foster, C. Smythe, G. Battaglia and J. A. Thomas, *Nat. Chem.*, 2009, **1**, 662–667; (c) M. R. Gill and J. A. Thomas, *Chem. Soc. Rev.*, 2012, **41**, 3179–3192; (d) J. Rodríguez, J. Mosquera, J. R. Couceiro, M. E. Vázquez and J. L. Mascareñas, *Angew. Chem., Int. Ed.*, 2016, **55**, 15615–15618; (e) B. C. Poulsen, S. Estalayo-Adrián, S. Blasco, S. A. Bright, J. M. Kelly, D. Clive Williams and T. Gunnlaugsson, *Dalton Trans.*, 2016, **45**, 18208–18220.
- (a) C. L. Kielkopf, K. E. Erkkila, B. P. Hudson, J. K. Barton and D. C. Rees, *Nat. Struct. Biol.*, 2000, **7**, 117–121; (b) H. Song, J. T. Kaiser and J. K. Barton, *Nat. Chem.*, 2012, **4**, 615–620.
- (a) A. E. Friedman, J. C. Chambron, J. P. Sauvage, N. J. Turro and J. K. Barton, *J. Am. Chem. Soc.*, 1990, **112**, 4960–4962; (b) H.-K. Liu and P. J. Sadler, *Acc. Chem. Res.*, 2011, **44**, 349–359.
- (a) P. Guo, A. A. Farahat, A. Paul, N. K. Harika, D. W. Boykin and W. D. Wilson, *J. Am. Chem. Soc.*, 2018, **140**, 14761–14769; (b) S. Neidle, *Nat. Prod. Rep.*, 2001, **18**, 291–309; (c) M. E. Vázquez, A. M. Caamaño, J. Martínez-Costas, L. Castedo and J. L. Mascareñas, *Angew. Chem., Int. Ed.*, 2001, **40**, 4723–4725; (d) O. Vázquez, M. E. Vázquez, J. B. Blanco, L. Castedo and J. L. Mascareñas, *Angew. Chem., Int. Ed.*, 2007, **46**, 6886–6890.
- (a) J. K. Barton, J. M. Goldberg, C. V. Kumar and N. J. Turro, *J. Am. Chem. Soc.*, 1986, **108**, 2081–2088; (b) C. V. Kumar, J. K. Barton and N. J. Turro, *J. Am. Chem. Soc.*, 1985, **107**, 5518–5523; (c) A. Papakyriakou, G. Malandrinos and A. Garoufis, *J. Inorg. Biochem.*, 2006, **100**, 1842–1848; (d) H. Ahmad, A. Wragg, W. Cullen, C. Wombwell, A. J. H. M. Meijer and J. A. Thomas, *Chem.–Eur. J.*, 2014, **20**, 3089–3096; (e) I. Gamba, I. Salvadó, G. Rama, M. Bertazzon, M. I. Sánchez, V. M. Sánchez-Pedregal, J. Martínez-Costas, R. F. Brissos, P. Gamez, J. L. Mascareñas, M. Vázquez López and M. E. Vázquez, *Chem.–Eur. J.*, 2013, **19**, 13369–13375.
- (a) A. Greguric, I. D. Greguric, T. W. Hambley, J. R. Aldrich-Wright and J. G. Collins, *J. Chem. Soc., Dalton Trans.*, 2002, 849–855; (b) H. Niyazi, J. P. Hall, K. O'Sullivan, G. Winter, T. Sorensen, J. M. Kelly and C. J. Cardin, *Nat. Chem.*, 2012, **4**, 621–628; (c) J. P. Hall, P. M. Keane, H. Beer, K. Buchner,



- G. Winter, T. L. Sorensen, D. J. Cardin, J. A. Brazier and C. J. Cardin, *Nucleic Acids Res.*, 2016, **44**, 9472–9482; (d) H. Song, J. T. Kaiser and J. K. Barton, *Nat. Chem.*, 2012, **4**, 615–620; (e) A. N. Boynton, L. Marcélis and J. K. Barton, *J. Am. Chem. Soc.*, 2016, **138**, 5020–5023.
- 8 A. C. Komor and J. K. Barton, *Chem. Commun.*, 2013, **49**, 3617–3630.
- 9 S. Neidle, *Nat. Prod. Rep.*, 2001, **18**, 291–309.
- 10 (a) C. Kaes, A. Katz and M. W. Hosseini, *Chem. Rev.*, 2000, **100**, 3553–3590; (b) T. Wang, N. Zabarska, Y. Wu, M. Lamla, S. Fischer, K. Monczak, D. Y. W. Ng, S. Rau and T. Weil, *Chem. Commun.*, 2015, **51**, 12552–12555; (c) E. Wachter, D. K. Heidary, B. S. Howerton, S. Parkin and E. C. Glazer, *Chem. Commun.*, 2012, **48**, 9649–9651.
- 11 (a) O. Vázquez, M. I. Sánchez, J. Martínez-Costas, M. E. Vázquez and J. L. Mascareñas, *Org. Lett.*, 2010, **12**, 216–219; (b) O. Vázquez, M. I. Sánchez, J. L. Mascareñas and M. E. Vázquez, *Chem. Commun.*, 2010, **46**, 5518–5520; (c) M. I. Sánchez, O. Vázquez, J. Martínez-Costas, M. Eugenio Vázquez and J. L. Mascareñas, *Chem. Sci.*, 2012, **3**, 2383–2387; (d) R. Nanjunda and W. D. Wilson, *Curr. Protoc. Nucleic Acid Chem.*, 2012, <https://currentprotocols.onlinelibrary.wiley.com/doi/abs/10.1002/0471142700.nc0808s51>; (e) E. Pazos, J. Mosquera, M. E. Vázquez and J. L. Mascareñas, *ChemBioChem*, 2011, **12**, 1958–1973.
- 12 (a) A. Paul, A. Kumar, R. Nanjunda, A. A. Farahat, D. W. Boykin and W. D. Wilson, *Org. Biomol. Chem.*, 2017, **15**, 827–835; (b) P. Guo, A. A. Farahat, A. Paul, N. K. Harika, D. W. Boykin and W. D. Wilson, *J. Am. Chem. Soc.*, 2018, **140**, 14761–14769.
- 13 (a) X. Hua and A. Von Zelewsky, *Inorg. Chem.*, 1991, **30**, 3796–3798; (b) X. Hua and A. von Zelewsky, *Inorg. Chem.*, 1995, **34**, 5791–5797; (c) M. Brissard, O. Convert, M. Gruselle, C. Guyard-Duhayon and R. Thouvenot, *Inorg. Chem.*, 2003, **42**, 1378–1385.
- 14 (a) C. Fu, M. Wenzel, E. Treutlein, K. Harms and E. Meggers, *Inorg. Chem.*, 2012, **51**, 10004–10011; (b) S. G. Telfer, T. M. McLean and M. R. Waterland, *Dalton Trans.*, 2011, **40**, 3097–3108.
- 15 (a) C. V. Kumar, J. K. Barton and N. J. Turro, *J. Am. Chem. Soc.*, 1985, **107**, 5518–5523; (b) M. R. Gill, H. Derratt, C. G. W. Smythe, G. Battaglia and J. A. Thomas, *ChemBioChem*, 2011, **12**, 877–880; (c) M.-J. Han, L.-H. Gao, Y.-Y. Lü and K.-Z. Wang, *J. Phys. Chem. B*, 2006, **110**, 2364–2371; (d) S. Arounaguirri and B. G. Maiya, *Inorg. Chem.*, 1999, **38**, 842–843; (e) C. Hiort, P. Lincoln and B. Norden, *J. Am. Chem. Soc.*, 1993, **115**, 3448–3454.
- 16 P. Thordarson, *Chem. Soc. Rev.*, 2010, **40**, 1305–1323.
- 17 (a) D. Roeland Boer, A. Canals and M. Coll, *Dalton Trans.*, 2008, 399–414; (b) C. Bailly and J. B. Chaires, *Bioconjugate Chem.*, 1998, **9**, 513–538; (c) B. S. Reddy, S. M. Sondhi and J. W. Lown, *Pharmacol. Ther.*, 1999, **84**, 1–111; M. A. Ismail, R. K. Arafa, R. Brun, T. Wenzler, Y. Miao, W. D. Wilson, C. Generaux, A. Bridges, J. E. Hal and D. W. Boykin, *J. Med. Chem.*, 2006, **49**, 5324–5332.
- 18 Although it has been reported that water-mediated contacts can compensate for poor shape complementarity, the length of the bipyridine ligand (more than 20 Å between the aminidium carbon atoms) would likely not allow the mechanism to operate. (a) B. Nguyen, S. Neidle and W. D. Wilson, *Acc. Chem. Res.*, 2009, **42**, 11–21; (b) B. Nguyen, M. P. H. Lee, D. Hamelberg, A. Joubert, C. Bailly, R. Brun, S. Neidle and W. D. Wilson, *J. Am. Chem. Soc.*, 2002, **124**, 13680–13681.
- 19 A. B. Tossi and J. M. Kelly, *Photochem. Photobiol.*, 1989, **49**, 545–556.
- 20 N. Holmgaard List, J. Knoops, J. Rubio-Magnieto, J. Idé, D. Beljonne, P. Norman, M. Surin and M. Linares, *J. Am. Chem. Soc.*, 2017, **139**, 14947–14953.
- 21 The changes in the CD spectra are different to those observed with intercalative complexes: S. D. Choi, M. S. Kim, S. K. Kim, P. Lincoln, E. Tuite and B. Nordén, *Biochemistry*, 1997, **36**, 214–223.
- 22 Circular dichroism experiments require high concentrations (5–10 times the  $K_{DS}$ ), which is why no differences are observed between  $\Delta$ -4Ru and  $\Lambda$ -4Ru using this technique.
- 23 T. A. Larsen, D. S. Goodsell, D. Cascio, K. Grzeskowiak and R. E. Dickerson, *J. Biomol. Struct. Dyn.*, 1989, **7**, 477–491.
- 24 Earlier studies have shown that DAPI is particularly suited for the study of DNA-binding complexes through competitive titrations: C. B. Spillane, J. A. Smith, J. L. Morgan and F. R. Keene, *J. Biol. Inorg. Chem.*, 2007, **12**, 819–824.
- 25 A. Rodger, G. Dorrington and D. L. Ang, *Analyst*, 2016, **141**, 6490–6498.
- 26 P. Lincoln, A. Broo and B. Nordén, *J. Am. Chem. Soc.*, 1996, **118**, 2644–2653.
- 27 D. Bouzada, I. Salvadó, G. Barka, G. Rama, J. Martínez-Costas, R. Lorca, Á. Somoza, M. Melle-Franco, M. E. Vázquez and M. Vázquez López, *Chem. Commun.*, 2018, **54**, 658–661.
- 28 L. Lercher, M. A. McDonough, A. H. El-Sagheer, A. Thalhammer, S. Kriaucionis, T. Brown and C. J. Schofield, *Chem. Commun.*, 2014, **50**, 1794–1796 (PDB ID: 4C64).
- 29 Data for  $[\text{Ru}(\text{bpy})_2\text{phen}]^{2+}$  from: P. Lincoln and B. Nordén, *J. Phys. Chem. B*, 1998, **102**, 9583–9594.
- 30 Model built with 3dna software: A. V. Colasanti, X.-J. Lu and W. K. Olson, *J. Visualized Exp.*, 2013, e4401.
- 31 (a) B. J. Pages, D. L. Ang, E. P. Wright and J. R. Aldrich-Wright, *Dalton Trans.*, 2015, **44**, 3505–3526; (b) C. Oguey, N. Foloppe and B. Hartmann, *PLoS One*, 2010, **5**, e15931; (c) S. Laughlin-Toth, E. K. Carter, I. Ivanov and W. D. Wilson, *Nucleic Acids Res.*, 2017, **45**, 1297–1306; (d) P. M. Keane, F. E. Poynton, J. P. Hall, I. V. Sazanovich, M. Towrie, T. Gunnlaugsson, S. J. Quinn, C. J. Cardin and J. M. Kelly, *Angew. Chem., Int. Ed.*, 2015, **54**, 8364–8368; (e) P. M. Keane, J. P. Hall, F. E. Poynton, B. C. Poulsen, S. P. Gurung, I. P. Clark, I. V. Sazanovich, M. Towrie, T. Gunnlaugsson, S. J. Quinn, C. J. Cardin and J. M. Kelly, *Chemistry*, 2017, **23**, 10344–10351; (f) J. P. Hall, F. E. Poynton, P. M. Keane, S. P. Gurung, J. A. Brazier, D. J. Cardin, G. Winter, T. Gunnlaugsson, I. V. Sazanovich,



- M. Towrie, C. J. Cardin, J. M. Kelly and S. J. Quinn, *Nat. Chem.*, 2015, **7**, 961–967.
- 32 C. Laughton and B. Luisi, *J. Mol. Biol.*, 1999, **288**, 953–963.
- 33 Molecular graphics obtained with UCSF Chimera, by the Resource for Biocomputing, Visualization, and Informatics at the University of California, San Francisco, with support from NIH P41-GM103311. E. F. Pettersen, T. D. Goddard, C. C. Huang, G. S. Couch, D. M. Greenblatt, E. C. Meng and T. E. Ferrin, *J. Comput. Chem.*, 2004, **25**, 1605–1612.
- 34 S. Sprouse, K. A. King, P. J. Spellane and R. J. Watts, *J. Am. Chem. Soc.*, 1984, **106**, 6647–6653.
- 35 J. N. Demas, E. W. Harris and R. P. McBride, *J. Am. Chem. Soc.*, 1977, **99**, 3547–3551.
- 36 M. B. Fleisher, K. C. Waterman, N. J. Turro and J. K. Barton, *Inorg. Chem.*, 1986, **25**, 3549–3551.

